Pergamon

Journal of Structural Geology, Vol. 16, No. 5, pp. 709 to 717, 1994

0191-8141/94 $07.00+0.00

Spider texture and amphibole preferred orientations

DAVID SHELLEY

Department of Geology, University of Canterbury, Private Bag 4800, Christchurch, New Zealand

(*Received* 15 *February* 1993; *accepted in revised form* 21 *June* 1993)

Abstract—Foliation in blueschist facies chert from California is defined by layers of oriented alkali-amphibole which consistently curve towards and converge on pyrite (and possibly pyrrhotite) crystals. These foliation nodes, not previously described, are called here 'spider texture'. The texture is interpreted in terms of perturbations of the stress field in a matrix undergoing strain about rigid pyrite (or pyrrhotite) crystals, and it has important implications for understanding the mechanisms of amphibole preferred orientation development. Geometrical relationships between spider texture, pressure shadows and quartz preferred orientations suggest that amphiboles grew with a strong preferred orientation along planes of maximum shearing stress. The mechanism of foliation and preferred orientation development probably involved competitive anisotropic growth of amphibole prisms within the small gaps that open at steps on shear planes, followed by additional (micro-) porphyroblastic growth. The first stage of the mechanism is similar to slickenfibre development.

INTRODUCTION TO AMPHIBOLE PREFERRED ORIENTATIONS

AMPHIBOLES in metamorphic rocks ranging from the blueschist and greenschist facies through the amphibolite facies often display very strong preferred orientations with *c*-axes (and prism lengths) parallel to, and defining, the lineation, and some of the best examples of linear schist have their structure dominated by and defined by oriented amphiboles. Despite the importance of amphibole preferred orientations in crustal rocks, few formal descriptions exist, and there are even fewer discussions of the origins of these fabrics. It seems appropriate, therefore, to present the following brief review, which draws together what information there is, before describing the spider texture and associated amphibole fabrics from California.

Formal descriptions of amphibole preferred orientations have shown:

(1) amphibole *c*-axes and long-axes define a lineation and/or foliation;

(2) either {110} is parallel to layering (Schwerdtner 1964, Gapais & Brun 1981), or {100} is parallel to layering (Rousell 1981, Hara *et al.* 1983, Mainprice & Nicolas 1989), or *b*-axes form a great circle about the lineation (Hara *et al.* 1983).

Typically the amphiboles are euhedral or subhedral, so it is common to see numerous euhedral sections with the characteristic amphibole shape in sections perpendicular to the lineation (Fig. 4a); in sections parallel to the lineation, prismatic sections typically show a strong alignment, possibly defining a planar foliation as well as the lineation. Even if amphiboles are clustered in mosaics, the subhedral character is often very much in evidence (Shelley 1992, fig. 7.29).

The following terminology, given in Shelley (1989, 1992), will be used throughout this paper to discuss the principal types of mechanism that may possibly cause amphibole preferred orientations to develop:

P-type: plastic deformation (dislocation creep, slip).

M-type: mechanical rotation of rigid inequidimensional crystals.

G-type: growth mechanisms, especially competitive anisotropic growth.

P-*type mechanisms*

Various slip and twin systems of the amphiboles have been investigated experimentally and/or in naturally deformed rocks by Dollinger & Blacic (1975), Rooney *et al.* (1975), Biermann (1981), Biermann & van Roermund (1983) and Cumbest *et al.* (1989a,b). Evidence of deformation twinning, bent crystals and sub-grain formation has been described from the blueschist, greenschist, amphibolite, granulite and eclogite facies. Despite these investigations into amphibole plasticity, it is generally acknowledged that amphiboles are the least plastic of the common rock-forming silicate minerals (Brodie & Rutter 1985), and evidence of plastic deformation is rare, especially in rocks of low grade. If amphiboles are embedded in a more plastic matrix, they are more likely to rotate during strain as rigid particles (Ildefonse *et al.* 1990), rather than deform plastically. Pervasive brittle fracturing, rather than plastic deformation, is noted by Allison & LaTour (1977) as the cause of an unusual preferred orientation with *c*-axes rotated away from the foliation due to rotation of fragments bounded by planes subnormal to *c*.

The formation of sub-grains and bending of amphiboles has been taken by some workers to indicate plastic deformation (e.g. Cumbest *et al.* 1989a), but observations of Nyman *et al.* (1992) on undulatory extinction in amphibole and sub-grains in core–mantle structure show that these features may be due to cataclasis, not plastic deformation. Similar cataclasis of feldspar with the production of 'sub-grains' and undulatory extinction is described by Tullis & Yund (1987). 'Recrystallization' of feldspar and amphibole, as distinct from the more

familiar recrystallization of quartz, involves chemical changes, and the possible driving forces therefore include a decrease in chemical free energy as well as strain. The 'recrystallization' discussed by Vernon (1975), White (1975) and Cumbest *et al.* (1989a), for example, may involve a classical nucleation process which blurs, therefore, the common distinction between what is 'crystallization' and 'recrystallization'.

Despite the evidence for plastic deformation in some rocks, not a single worker, to my knowledge, has been able to link the generation of natural amphibole preferred orientations to plastic deformation, though the possibility is mooted by Mainprice & Nicolas (1989). Indeed, given that amphibole is nearly always the least plastic mineral in a rock, the likelihood of *P*-type fabrics being produced seems remote. In those common amphibole-bearing rocks, such as those to be described here, where amphiboles occur as euhedral or subhedral crystals, often spaced from neighbouring euhedral crystals (Fig. 4a), it is clear that *P*-type mechanisms had no essential role in producing their preferred orientation.

M-*type mechanisms*

The concept that amphibole prisms can be rotated as rigid particles into a preferred orientation by strain of a more plastic matrix is favoured by Hara *et al.* (1983) for 'older' amphiboles in the rocks they describe, suggested as a strong possibility by Mainprice & Nicolas (1989), and as a probability by Ildefonse *et al.* (1990).

The glaucophane-bearing schists of Ildefonse *et al.* (1990) provide the only explicit documentation of the possible operation of an *M*-type mechanism. The principal evidence is a positive correlation between the intensity of amphibole preferred orientation (documented by rose-diagrams of grain-length orientation) and amphibole aspect ratio: the more elongate the glaucophane, the stronger the preferred orientation. Evidence for the *M*-type process also includes pressure shadows around the amphiboles and boudinage of amphibole, which suggests that the matrix of quartz and mica was plastic, whereas the amphibole was not.

G-*type mechanisms*

An explanation of amphibole preferred orientations by competitive anisotropic growth is favoured by Hara *et al.* (1983) for the 'newer' amphiboles in the rocks they describe, and by Schwerdtner (1964) and Brodie & Rutter (1985). Schwerdtner (1964) advocates a mechanism whereby the strongest axis (*c*) grows preferentially in the direction of the minimum principal stress axis, as proposed by Kamb (1959). However, the efficacy of this mechanism has not generally been supported in the recent literature, and Helmstaedt *et al.* (1972), for example, show that the preferred orientations of amphibole and pyroxene in adjacent layers are inconsistent with application of the Kamb theory. Brodie & Rutter (1985) write of amphiboles that grow mimetically along pre-existing schistosity, and amphibole fibres that are produced by competitive anisotropic growth parallel to the dilation direction in opening spaces. Growth under stress is advocated by Hara *et al.* (1983), but not clearly explained.

The increasing recognition that solution transfer processes are capable of producing substantial general strain, including 'stretched conglomerates' (Norris & Bishop 1990), points to the probability that competitive anisotropic growth (which is the usual complement of pressure solution in solution transfer) is important in producing mineral preferred orientations. The potential was outlined clearly by Cox & Etheridge (1983), and such *G*-type mechanisms are discussed further in Shelley (1992). Some of the evidence of Ildefonse *et al.* (1990) could possibly be re-examined in terms of *G*-type mechanisms. For example, competitive anisotropic growth could also produce a positive correlation between a preferred orientation of euhedral grain-lengths and aspect ratio. Clearly, in the case of oriented, spaced amphibole crystals in a 'plastic' matrix, the possibilities of both *G*-type and *M*-type mechanisms need to be considered.

In the case of oriented subhedral amphiboles that are clustered together (Shelley 1992, fig. 7.29), it is clear that the final fabric and texture is achieved by the growing together of already oriented amphibole, possibly in combination with some competitive anisotropic growth mechanism. The difficult, often imponderable question, remains: 'How was the preferred orientation *initiated*?' Is the answer competitive anisotropic growth, so that crystals with *c*-axes parallel to opening or stretching directions were able to outgrow all others? Or were the initial embryo crystals rotated by strain of a ductile matrix (*M*-type mechanism), with subsequent growth responsible only for grain enlargement?

Spider texture, described for the first time below, provides an answer to this normally imponderable question.

SPECIMEN DESCRIPTION

The metacherts described here come from the Pickett Peak terrane within the blueschist facies Eastern Franciscan Belt of California. They are associated with metabasalt pillow lavas, exposed in a cutting on the Riley Ridge Road (grid reference EV 2719, 1:250,000 Ukiah Sheet NJ 10-2). Lineations, defined by amphibole, plunge at moderate angles to the east. The general geological setting and an interpretation of deformational history is given by Jayko & Blake (1989).

Specimen A13 consists of a recrystallized mosaic of quartz, of the order of 0.1 mm grain size, embedded in which are euhedral alkali-amphibole prisms with an extremely strong preferred orientation (Fig. 4a). The amphiboles range in size from <0.01 mm to approximately 0.1 mm along the *a*-axis, and up to 1.2 mm along the *c*-axis. The amphibole makes up approximately 10% of the rock, and whilst some of it is completely dispersed within the quartz, most of it is concentrated in layers

with a spacing in the range 0.1–1.0 mm. These layers typically are only as thick as one or two amphibole prisms. The amphibole has a pleochroic scheme α = yellow–brown, β and γ = intense dark blue (almost opaque), and the opaque character prevents routine optical determinations from being made. Infrequent, completely weathered pseudomorphs of euhedral pyrite crystals, typically up to 0.4 mm size, are scattered throughout. The pyrite is entirely replaced by goethite and limonite.

Specimen A17 also consists of alkali-amphibole and a recrystallized mosaic of quartz, and both the amphibole and quartz have a similar range of grain-sizes to those in A13. Similarly the alkali-amphibole has an extremely strong preferred orientation. However, in this specimen, the amphibole is more abundant but less evenly distributed, and forms not only completely dispersed euhedral prisms and thin layers within the quartz, but also layers up to 1 mm thick. Green aegirine, which predates the amphibole, is also present. Some of the amphibole in A17 has the typical glaucophane pleochroism including pale blue and lavender colours, but much of it has the same almost opaque blue colour as that in A13. Infrequent euhedral pyritohedral pyrite crystals, typically up to 1.5 mm size, are scattered throughout. Patches of unaltered pyrite do occur in A17, but most is replaced by goethite and limonite. Some of the crystals do not appear to have the shape of pyrite, and may possibly have been pyrrhotite.

Amphibole and quartz preferred orientations and structures

In both specimens, the amphibole preferred orientation is extremely strong. Because of the almost opaque character of much of the amphibole, standard U-stage optical determination of X, Y and Z axes is not feasible. However, in sections perpendicular to lineation, almost all amphiboles can be rotated into a position so that the b-axis is horizontal N–S, and the c-axis vertical. With the polarizer set E–W, this is easily judged from the euhedral shape, sharp cleavages and the relatively pale-brown colour (α is E–W) displayed by crystals in this orientation.

In A13 (Figs. 1a & b), amphibole c-axes form a strong maximum that defines the lineation, and which also by definition lies in the foliation. There is a slight spread of c-axes along the foliation. The b-axes concentrate as a maximum in the foliation, perpendicular to the lineation, with a tendency to spread as a girdle about the lineation. The two maxima symmetrical to foliation result from gentle crenulation-like structures affecting the foliation with axes parallel to the lineation. They do not result from {110} rather than {100} being parallel to foliation (both orientations have been reported in the literature—see Introduction), since the angle between the maxima is 30°.

In A17 (Figs. 1c & d), amphibole c-axes again form a simple maximum that defines the lineation. This specimen is characterized by a much more intense

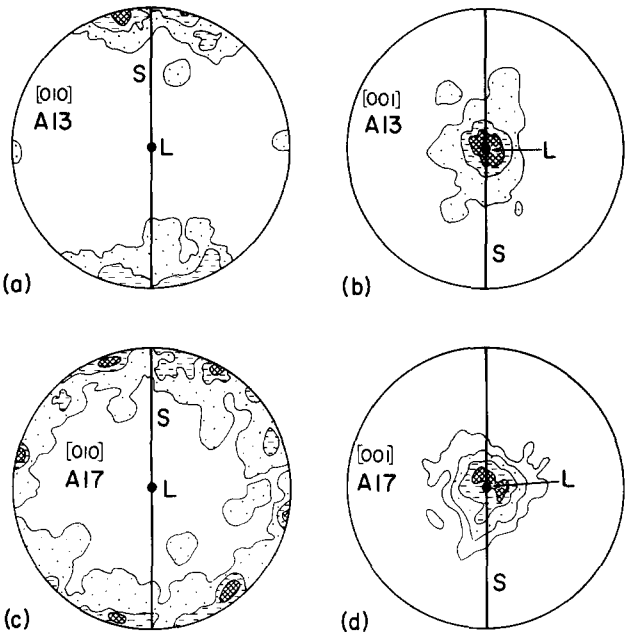

Fig. 1. Lower-hemisphere equal-area projections showing the preferred orientation of amphibole b-axes and c-axes in A13 and A17. Each diagram represents 100 measurements. S = foliation, L = lineation. Contours in (a) 2, 5 and 10% per 1% area (maximum 14%), in (b) 2, 8 and 14% per 1% area (maximum 26%), in (c) 1, 3 and 5% per 1% area (maximum 8%) and in (d) 2, 5, 10 and 15% per 1% area (maximum 20%).

crenulation-like structure with axes parallel to the lineation (Fig. 2), and this is reflected in the b-axes diagram which shows a girdle about the lineation.

In both specimens the foliation is discontinuous and anastomosing, particularly in sections perpendicular to the lineation where the crenulation-like structure is seen. In neither specimen is there clear evidence that the crenulations post-date the progressive development of

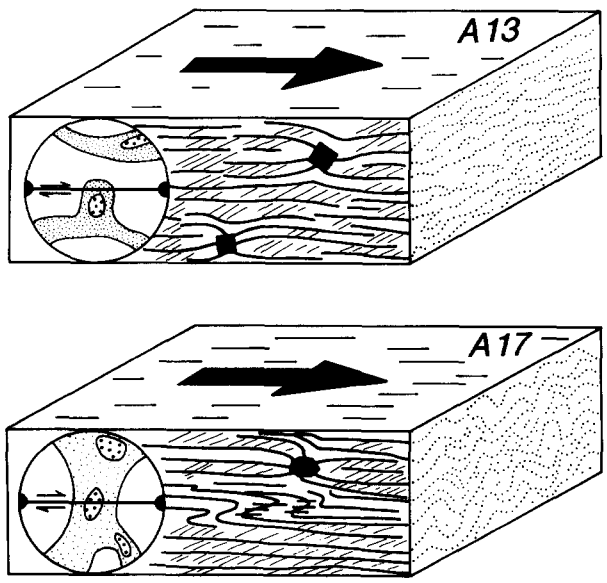

Fig. 2. Block diagrams that illustrate the principal structures in A13 and A17. The quartz grain elongation at a moderate angle to the foliation defined by oriented amphiboles, and diagrammatic representations of the quartz c-axes preferred orientations (cf. Fig. 3) are shown in the sections normal to the foliation and parallel to the lineation. The arrows indicate the sense of shear.

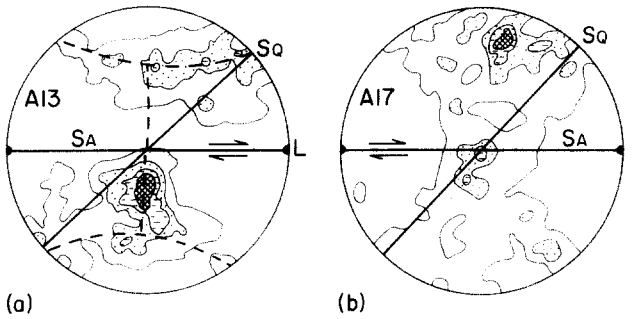

Fig. 3. Lower-hemisphere equal-area projections showing the preferred orientation of quartz *c*-axes in A13 and A17. Diagram (a) represents 800 measurements and (b) 300. SA = foliation defined by amphibole, SQ = grain-shape elongation of quartz and *L* = lineation. In (a) the skeleton of the type-1 crossed girdle pattern is highlighted by the dashed line. Contours in (a) and (b), 1, 2, 3 and 4% per 1% area (maximum 5%).

the quartz and amphibole textures and layering. The simpler interpretation is that both specimens are *S–L* tectonites with A13 closer to the *S*-tectonite end of the spectrum, and A17 closer to the *L*-tectonite end. In both cases, one can speculate that the crenulations developed as an integral part of the same strain that produced the lineation and foliation, but with a relatively larger and significant amount of shortening along the intermediate strain axis in A17.

In both specimens, quartz forms mosaics of dynamically recrystallized grains that are either sub-equidimensional or elongate at 40–50° to the foliation in the plane that contains the lineation and pole to the foliation (Fig. 4b). Quartz *c*-axes form a type-1 crossed-girdle pattern in A13, and are concentrated in the plane perpendicular or almost perpendicular to the lineation and foliation in A17 (Fig. 3). The quartz fabrics are similar to those described from mylonitic rocks (e.g. Law *et al.* 1986, Law 1990), and can be interpreted to represent dynamic recrystallization during a deformation that approximated a simple shear, with the amphibole foliation representing the shear plane (equivalent to a mylonitic *C*-surface), and the quartz elongation the final increment of strain (Figs. 2 and 4b). The contrast between small circles of quartz *c*-axes in A13 and the single great circle pattern of A17 is consistent with the suggestion above that A13 and A17 are, respectively, closer to the *S* and *L* ends of the *S–L* tectonite spectrum.

In A17, tight to isoclinal folds of the foliation deform early-formed amphiboles, but developed contemporaneously with later amphiboles (Figs. 2 and 4c). Vergence of the folds is consistent with the sense of shear suggested by the general quartz fabric.

Quartz pressure shadows of the face-controlled type (Ramsay & Huber 1983) developed about pyrite (Figs. 4d & e). The shadows are elongate in directions that vary from approximately 45° to foliation, and parallel to the general quartz grain elongation direction, to almost parallel to the foliation. In some cases the fibrous nature of the shadow can still be discerned, but in others it is obscured or destroyed by dynamic recrystallization.

SPIDER TEXTURE

Valuable insight into the reasons for the development of amphibole preferred orientation is provided by perturbations of foliation adjacent to pyrite crystals. In these regions, the amphibole foliation consistently curves towards and converges on pyrite crystals, and the distinctive texture that results (Figs. 4d and 5) does not appear to have been described before. I will call it 'spider texture'.

Before reaching a decision on how to interpret spider texture, it is worth examining some ideas that prove not to be valid. Firstly, the curving of amphibole towards pyrite is mimicked by some of the patterns produced by Ildefonse *et al.* (1992) as digitally-derived representations of experimental simple shear. These patterns are only visible immediately adjacent to elongate rigid particles with their lengths set initially at high angles to the shortening direction. Importantly, Ildefonse *et al.* (1992) state that patterns immediately adjacent to rigid particles "are not significant", and what they do regard as significant are the zones of high strain that develop along the finite strain elongation direction (either side of the rigid particle). Apart from the implication that the spider texture patterns of Ildefonse *et al.* (1992) may be an artefact of the experiment, the spider texture described here differs in a number of respects. In particular, most pyrites are equidimensional, and there is no suggestion of a high strain zone to the sides of the pyrites (Figs. 4d and 5b). The more familiar strain patterns near rigid crystals in natural rocks and other experiments are, in fact, very different from spider texture. Micas that 'wrap-around' rigid garnets in schist provide one example, and similar patterns also feature in the experiments of Ghosh (1975) and Van Den Driessche & Brun (1987).

Secondly, some examples of spider texture resemble boudinage, where typically the foliation surfaces curve in towards the site of separation. It seems unlikely that rigid pyrite crystals would act as nuclei for boudinage, but one should perhaps consider the possibility that the pyrite post-dates the general perturbation of foliation, and developed at the sites of parting. The idea, however, falls down because the texture occurs in both quartz and amphibole-rich layers, and apart from the spider itself, there is no suggestion of boudinage at nearby layer boundaries (Figs. 5b & c).

Thirdly, the texture resembles some face-controlled fibrous pressure-shadow patterns. However, many of the pyrite crystals display face-controlled patterns of quartz fibres, and in general the quartz and amphiboles are not parallel (Figs. 4d and 5b & d). The development of quartz fibres and amphibole prisms overlap in time, so that some amphiboles are displaced by quartz (Fig. 5d) whereas others cut obliquely across and post-date the quartz (Fig. 4d). There is some resemblance to the displacement-controlled fibres that develop synchronously with, but cut across, face-controlled fibres, as described by Ramsay & Huber (1983, figs. 14.10–14.12). However, the overall form of most spider textures is not

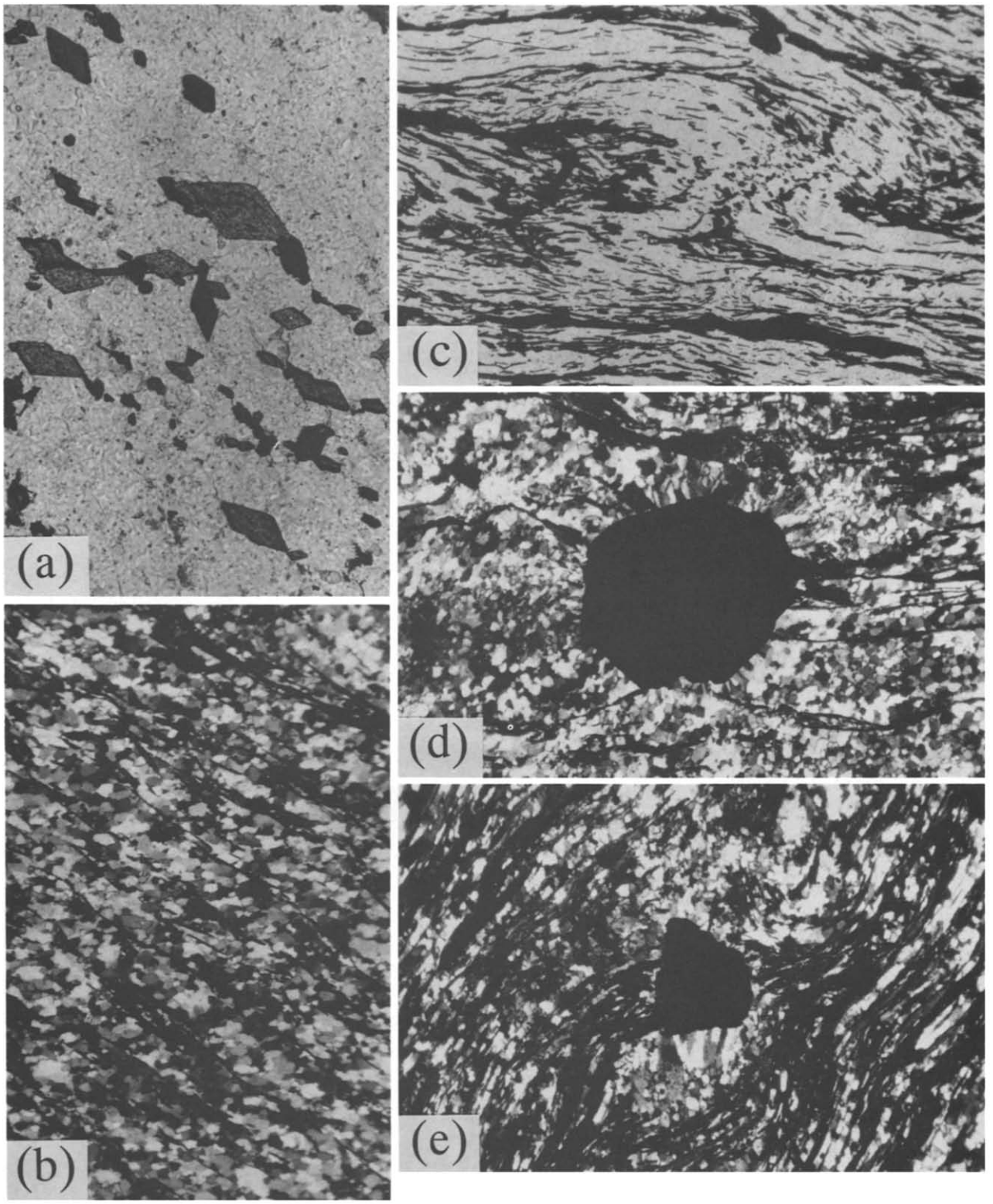

Fig. 4. (a) Alkali-amphibole set in quartz in metachert (specimen A13 from California) cut perpendicular to lineation. Discrete euhedral alkali-amphibole crystals display a very strong preferred orientation. (b) Metachert specimen A13 in a section parallel to the lineation. Alkali-amphibole defines the dark, thin, discontinuous, anastomosing foliation structure, and the dynamically recrystallized quartz has a weak grain elongation (E–W in the photograph), 40° to the amphibole foliation. (c) Tight to isoclinal folding of the amphibole foliation in specimen A17 in a section parallel to lineation and at a high angle to fold axes. A new orientation of amphibole and small displacements along the direction of the new amphibole prisms can be seen in parts of the hinge zone (centre to centre-right of photograph). (d) Pyritohedron in A17 showing spider texture and a face-controlled fibrous quartz pressure shadow. Amphibole foliation is seen as thin dark lines which converge on or curve towards the pyrite, and which are often at an angle to, and cut across quartz fibres (clearly seen at the pyrite base). (e) Pyrite with fibrous quartz pressure shadow at a moderate angle to the amphibole foliation. The pyrite is displaced dextrally with respect to an earlier part of the pressure shadow, and a curved region of foliation, above and to the right of the pyrite, represents an earlier formed spider texture displaced dextrally relative to the pyrite. The displacements are shown again in Fig. 6 for clarity. View lengths are 0.83 mm in (a) and 3.2 mm in (b)–(e). (a) & (c) are in ppl; (b), (d) & (e) in cpl.

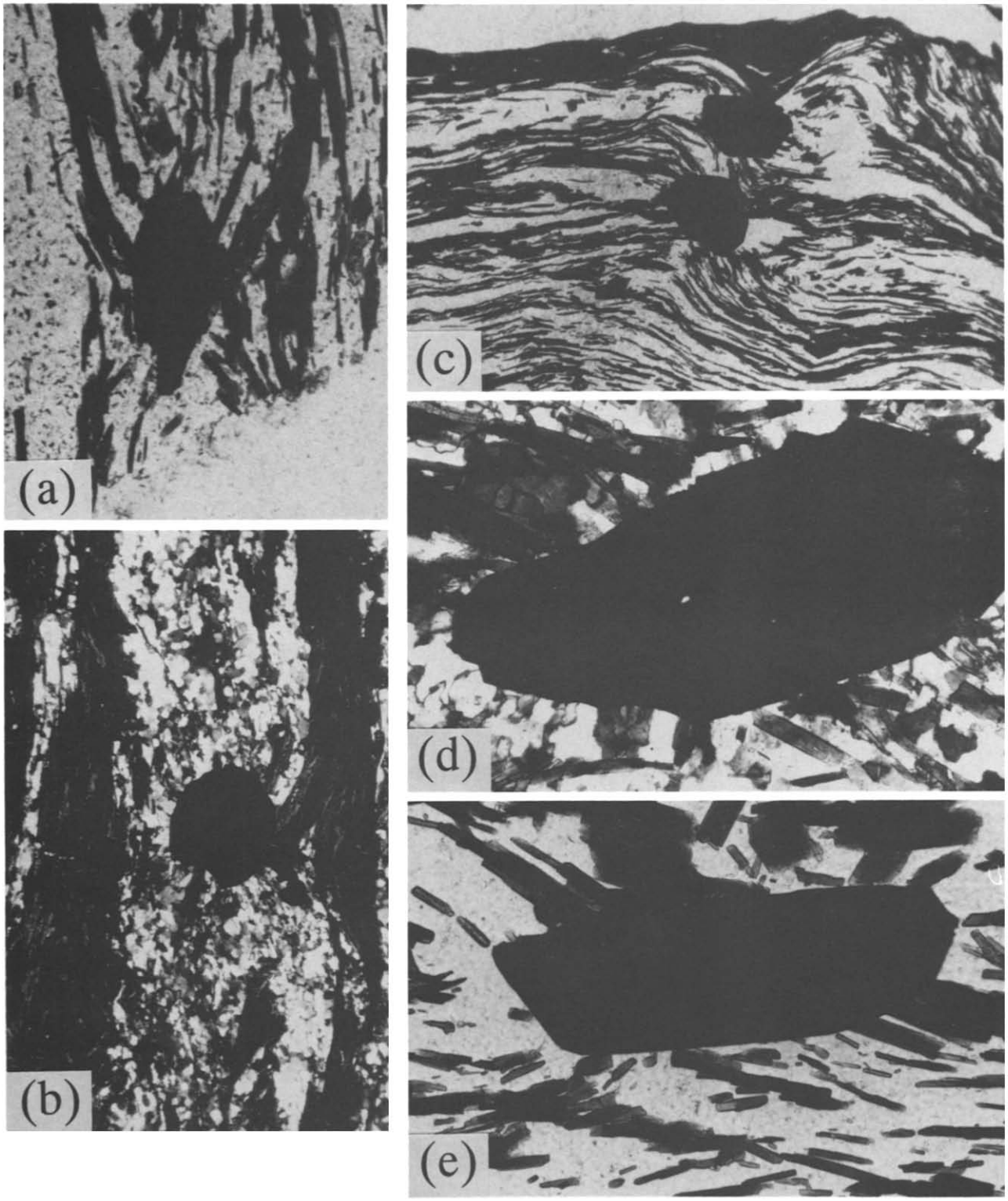

Fig. 5. (a) Spider texture in A17 showing amphibole prisms that curve towards and converge on a crystal which in this case may have been pyrrhotite. The edge of the slide is seen towards the bottom. (b) Spider texture in A17 involving relatively thick layers of amphibole and showing the simple planar foliation surfaces (i.e. a lack of boudinage) away from the immediate vicinity of the spider texture. (c) A double example of spider texture in A17 involving both thick and thin amphibole layers. Note again the lack of boudinage affecting the amphibole–quartz boundary (at the top). (d) Detail of spider texture in A17 showing lack of parallelism of quartz fibres and amphibole prisms (clearly seen at base where a curved amphibole foliation trace and amphibole oblique to the pyrite faces are discordant to or cross-cut the quartz fibres (which are perpendicular to the pyrite faces). At the top, the latest stage of quartz fibre growth adjacent to the pyrite has clearly displaced earlier obliquely oriented amphiboles. (e) Spider texture in A17 showing the development of amphibole with a new orientation from pre-existing prisms that define the foliation in the bottom left of the picture. The pyrite has probably been displaced dextrally relative to the amphibole foliation below it which represents an earlier stage of spider texture formation. View lengths measure 1.2 mm in (a), 3.2 mm in (b) & (c) and 0.83 mm in (d) & (e). (a), (c) & (e) are in ppl; (b) & (d) in cpl.

the same as the contact suture between pressure shadow and matrix, as should be the case.

Fourthly, Figs. 4(d), 5(b) & (c) show foliation surfaces with continuous curves that are convex towards the pyrite, but which never contact the pyrite. This geometry is incompatible with a mechanism involving divergent epitaxial fibre growth on the pyrite combined with subsequent rotation during strain.

Fifthly, the texture superficially resembles some of the complex patterns produced in shear-zone experiments by Ghosh (1975, figs. 12 and 13) where pre-existing markers more-or-less parallel to the shortening direction form a pattern about rigid bodies rather similar to spider texture. Given that the marker lines of Ghosh could represent some pre-existing fabric, the possibility of spider texture developing because of multiphase deformation and a progressive reorientation of amphibole fabrics needs to be addressed. Is it possible, for example, that the spiders are really millipedes in the sense of Bell & Rubenach (1980)? With reference to the Ghosh shear zone model, the principal problem is the relationship between spider texture and the preferred orientation of the quartz. According to this model, the spider texture and grain shapes of quartz would have developed in a sinistral shear zone, at a high angle to and complementary to the dextral shear zone shown in Fig. 2. However, this is completely incompatible with the girdles of quartz *c*-axes which are consistent only with the dextral shear proposed. With regard to millipede textures and structures, the essential difference is that the rigid central part of the millipede contains the relics of a pre-existing mineral fabric, either as an inclusion trail or as a microlithon (Bell & Rubenach 1980). There is no equivalent to this in the spider texture. More importantly, however, the fact that the curved trails of amphiboles intersect undeformed fibrous pressure shadows of quartz (Figs. 4d and 5b & d) seems to rule out any possibility of the spiders representing multiphase deformation.

Perturbation of the stress field

What seems more likely is that spider texture represents a perturbation of one of the planes of maximum shearing stress in a somewhat plastic matrix deformed about a rigid object. The following model is developed in terms of typical shear zone geometry.

The walls of an ideal brittle or ductile shear zone are initiated parallel to one of the planes of maximum shearing stress, and mineral fabrics within the shear zone will define finite or incremental strains so that grain lengths preferentially lie somewhere in the zone between perpendicular to the shortening direction and parallel to the shear zone wall. In the case of *S*–*C*-mylonites, the *C*-planes (from the French *cisaillement*, or shearing) are subparallel to the shear zone wall whereas the *S*-planes are at higher angles to the shortening direction (Simpson 1986). Both planes are defined by grain shape preferred orientations. The strain field within a ductile shear zone is perturbed adjacent to rigid bodies, well illustrated by the way quartz ribbons and micas are wrapped around rigid feldspar porphyroclasts or garnet crystals in mylonites and schists, for example. Such perturbations are a feature of models in which the rigid body rotates (Ghosh 1975, Van Den Driessche & Brun 1987) as well as models where the rigid body does not rotate (Bell & Johnson 1992). For a small strain increment there is a simple relationship between stress and strain so that the two planes of maximum shearing stress are at moderate angles and symmetrical to the incremental shortening and extension directions. Thus, if the strain field is perturbed about a rigid body in a shear zone so too are the positions of the planes of maximum shearing stress. Shearing in any one shear zone is dominated by only one of the two planes of maximum shearing stress, and it is shown in Fig. 7 that the smooth trajectories of this plane (solid lines drawn at a moderate angle to the incremental extension directions) curve in towards and converge on any rigid object.

The fabrics of A13 and A17 are consistent with this shear zone model so that: (1) amphiboles are oriented along the shear planes, similar to the *C*-planes of mylonites; (2) the quartz grain lengths represent some late increment of strain during dynamic recrystallization, similar to the *S*-planes of mylonites; and (3) pressure shadows lie somewhere in the zone between the quartz shape preferred orientation and the shear planes. Consistent with this model are the occasional observations of actual displacement (Figs. 4c & e and 6), in association with both shear-fold and pressure-shadow development. In most cases, the amount of displacement seems very small. Spider textures, the tight folds and the crenulations parallel to lineation, all represent some degree of heterogeneity and/or departure from the simple shear geometry of an ideal shear zone.

The proposed model of amphibole prism growth along shear planes is consistent with the more general observation that shear surfaces are commonly coated with fibrous growths, elongate in the direction of movement, called slickenfibres. Competitive anisotropic growth processes during fibre or prism growth are ex-

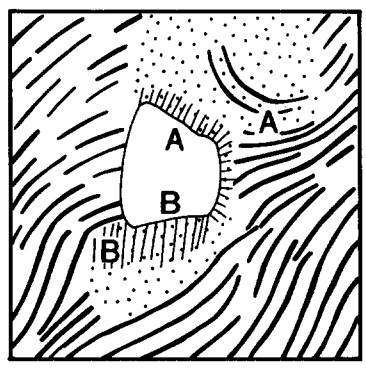

Fig. 6. A tracing from part of Fig. 4(e) to illustrate more clearly the displacements shown. Quartz pressure shadows are stippled, fibrous parts are finely lined, and the other parts are recrystallized. The orientation of amphibole prisms is represented by thick lines. Older, recrystallized areas of pressure shadow at A and B have been displaced dextrally and were originally close to the positions marked A and B within the pyrite. The recrystallized pressure shadow at A contains a curved pattern of amphibole prisms, a relic of a spider texture that formed when this area of pressure shadow was closer to the pyrite.

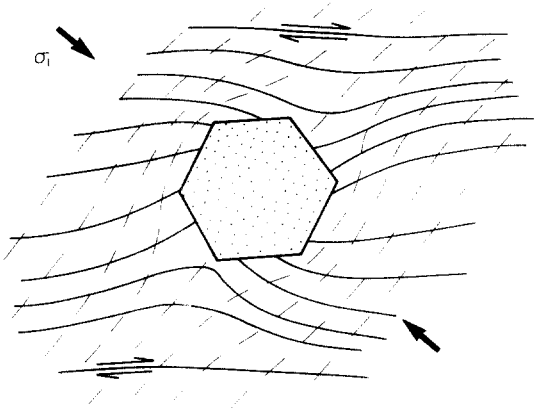

Fig. 7. Diagram that illustrates the perturbation of planes of maximum shearing stress (solid lines) in the vicinity of a solid object. The dashed lines represent extension directions during an infinitesimal strain (to which the solid lines make an angle of 45°), and the arrows represent the orientation of σ_1, the maximum principal compressive stress direction.

tremely efficient at eliminating less than ideal orientations (well illustrated not only by slickenfibres, but by fibrous vesicle infillings and quartz veins). Crystals grow along a shear surface because dilation occurs on small steps that inevitably form during failure. The orientation of fibre length is intrinsically related to this dilation and the opening direction.

If this interpretation of spider texture is correct, then it would seem that a *G*-type mechanism is responsible for the amphibole preferred orientation and that it originates at a very early stage of growth.

Progressive developments during amphibole crystallization

Naturally enough, the development of the metachert structures and the quartz and amphibole preferred orientations took place over a period of time, and did not develop instantaneously. Thus, here, I speculate that the crenulations with axes parallel to lineation are part and parcel of the same deformation that produced the foliation and lineation. The relative strengths of foliation and lineation, and the presence or absence of crenulations depend on the relative amounts of shortening along the intermediate strain axis. Similarly, the non-coaxial deformation indicated by the textures is compatible with the development of tight to isoclinal folds in a heterogeneous rock. The fact that some early amphiboles are caught up in such folds (Fig. 4c), and that further amphibole crystallization occurred after the folds formed should not be surprising, and should not necessarily lead to the definition of separate stages of deformation.

The progressive growth of amphibole can be seen, not only in the tight shear folds, but also in the displacement along the amphibole foliation of early-formed parts of pressure shadows (Figs. 4e and 6), and in some progressive changes to the spider pattern. For example, Fig. 5(e) illustrates the re-orientation of amphiboles at an angle to the pre-existing foliation, probably as a consequence of displacement during shearing of that foliation region past the pyrite, and the establishment of a new stress field, to which the amphibole very quickly responded. Similarly, in Figs. 4(e) and 6, a curved region of foliation, above and to the right of the pyrite, represents an earlier-formed portion of a spider texture that has been displaced dextrally relative to the pyrite. As in Fig. 5(e), close examination shows some amphibole in this region is re-oriented in response to the changed position of the pyrite.

The predicted asymmetric pattern of planes of maximum shearing stress, perturbed around rigid crystals (Fig. 7), is very similar to some of the spider texture (especially Fig. 5c, for example). The sense of asymmetry, when present, is always the same and consistent with Fig. 7, but the degree of asymmetry is not always as pronounced (e.g. Fig. 5a). The explanation may in part be that early spider textures are modified (essentially flattened) during progressive strain of the quartz matrix, or it may be due to the fact that Fig. 7 represents a snapshot view and simplification of the real situation. For example, spider textures are intimately associated with quartz pressure shadows which they cut, and by which they may be displaced, complications not modelled in Fig. 7.

The actual visible amounts of displacement associated with the crystallization of amphiboles, for example in association with folds (Fig. 4c) or the progressive development of some spiders (Fig. 5e), are often small, but evidently sufficient for embryonic crystals to develop a preferred orientation. Many amphibole prisms are longer than the possible amount of displacement, and this suggests that crystals that form first in dilational regions along shear planes, then continue to grow, encroach on shear-zone walls, and obscure the exact shear-surface traces.

CONCLUSIONS AND DISCUSSION

The textures, structures, and preferred orientations in specimens of Franciscan metachert from the Pickett Peak terrane can be interpreted in terms of one single progressive shear deformation in which amphiboles grew along planes of maximum shearing stress, essentially like slickenfibres followed by further porphyroblastic growth. Between surfaces of discrete shear failure, the accompanying quartz was deformed plastically and underwent dynamic recrystallization. The final increments of strain are recorded in the elongation of quartz. The secondary quartz and amphibole-rich layers were occasionally folded isoclinally during progressive shear, and new amphiboles quickly developed new orientations in response. Crenulations parallel to the lineation are an intrinsic part of the fabric, and relate to the relative values of the principal strains rather than secondary folding of the foliation.

A new texture, called here 'spider texture', is formed by the amphibole foliation which curves towards and converges on rigid pyrite crystals. The texture rep-

resents perturbations of the planes of maximum shearing stress adjacent to the rigid pyrite, and it enables a clear choice to be made between *M*-type and *G*-type mechanisms for the development of the amphibole preferred orientation. The spider texture requires an interpretation in terms of competitive anisotropic growth along shear planes (where dilation inevitably occurs). Without the information gleaned from spider texture it would be possible to argue that rigid amphibole prisms had been rotated as passive objects in plastic quartz until they were parallel or nearly parallel with the shear plane. Nevertheless, it would be difficult to explain the concentration of amphiboles in secondary layers by an *M*-type process.

How common is spider texture is a question still to be answered. A preliminary examination of specimens at the University of Canterbury has revealed only one other example, where a sheet-silicate foliation is perturbed adjacent to pyrite crystals in metacherts from the Caples terrane in Otago, New Zealand.

Acknowledgements—I wish to thank the University of Canterbury for providing a period of leave during which the specimens from California were collected, and in particular I wish to express my thanks to Clark Blake for introducing me to the Franciscan. My thanks too to Jocelyn Campbell for providing a glimpse of the metacherts from the Caples terrane in New Zealand, and to her, Gérard Bossière and Denis Gapais for discussing this paper.

REFERENCES

Allison, I. & LaTour, T. E. 1977. Brittle deformation of hornblende in a mylonite: a direct geometrical analogue of ductile deformation by translation gliding. *Can. J. Earth Sci.* **14**, 1953–1958.

Bell, T. H. & Johnson, S. E. 1992. Shear sense: a new approach that resolves conflicts between criteria in metamorphic rocks. *J. metamorph. Geol.* **10**, 99–124.

Bell, T. H. & Rubenach, M. J. 1980. Crenulation cleavage development—evidence for progressive bulk inhomogeneous shortening from "millipede" microstructures in the Robertson River Metamorphics. *Tectonophysics* **68**, T9–T15.

Biermann, C. 1981. (100) deformation twins in naturally deformed amphiboles. *Nature* **292**, 821–823.

Biermann, C. & van Roermund, H. L. M. 1983. Defect structures in naturally deformed clinoamphiboles—a TEM study. *Tectonophysics* **95**, 267–278.

Brodie, K. H. & Rutter, E. H. 1985. On the relationship between deformation and metamorphism, with special reference to the behavior of basic rocks. In: *Metamorphic Reactions—Kinetics, Textures, and Deformation* (edited by Thompson, A. B. & Rubie, D. C.). Springer, New York, 138–179.

Cox, S. F. & Etheridge, M. A. 1983. Crack-seal fibre growth mechanisms and their significance in the development of oriented layer silicate microstructures. *Tectonophysics* **92**, 147–170.

Cumbest, R. J., Drury, M. R., van Roermund, H. L. M. & Simpson, C. 1989a. Dynamic recrystallisation and chemical evolution of clinoamphibole from Senja, Norway. *Contr. Miner. Petrol.* **101**, 339–349.

Cumbest, R. J., van Roermund, H. L. M., Drury, M. R. & Simpson, C. 1989b. Burgers vector determination in clinoamphibole by computer simulation. *Am. Miner.* **74**, 586–592.

Dollinger, G. & Blacic, J. D. 1975. Deformation mechanisms in experimentally and naturally deformed amphiboles. *Earth Planet. Sci. Lett.* **26**, 409–416.

Gapais, D. & Brun, J. P. 1981. A comparison of mineral grain fabrics and finite strain in amphibolites from eastern Finland. *Can. J. Earth Sci.* **18**, 995–1003.

Ghosh, S. K. 1975. Distortion of planar structures around rigid spherical bodies. *Tectonophysics* **28**, 185–208.

Hara, I., Shiota, T., Maeda, M. & Miyaoka, H. 1983. Deformation and recrystallisation of amphiboles in Sanbagawa Schist with special reference to history of Sanbagawa metamorphism. *J. Sci. Series C: Geol. & Miner., Hiroshima Univ.* **8**, 135–148.

Helmstaedt, H., Anderson, O. L. & Gavasci, A. T. 1972. Petrofabric studies of eclogite, spinel–websterite, and spinel–lherzolite xenoliths from kimberlite-bearing breccia pipes in southeastern Utah and northeastern Arizona. *J. geophys. Res.* **77**, 4350–4365.

Ildefonse, B., Lardeaux, J. M. & Caron, J. M. 1990. The behavior of shape preferred orientations in metamorphic rocks: amphiboles and jadeites from the Monte Mucrone area (Sesia-Lanzo zone, Italian Western Alps). *J. Struct. Geol.* **12**, 1005–1011.

Ildefonse, B., Sokoutis, D. & Mancktelow, N. S. 1992. Mechanical interactions between rigid particles in a deforming ductile matrix. Analogue experiments in simple shear flow. *J. Struct. Geol.* **14**, 1253–1266.

Jayko, A. S. & Blake, M. C., Jr. 1989. Deformation of the Eastern Franciscan Belt, northern California. *J. Struct. Geol.* **11**, 375–390.

Kamb, W. B. 1959. Theory of preferred orientation developed by crystallisation under stress. *J. Geol.* **67**, 153–170.

Law, R. D. 1990. Crystallographic fabrics: a selective review of their applications to research in structural geology. In: *Deformation mechanisms, Rheology and Tectonics* (edited by Knipe, R. J. & Rutter, E. H.). *Spec. Publs. geol. Soc. Lond.* **54**, 335–352.

Law, R. D., Casey, M. & Knipe, R. J. 1986. Kinematic and tectonic significance of microstructures and crystallographic fabrics within quartz mylonites from the Assynt and Eriboll regions of the Moine thrust zone, NW Scotland. *Trans. R. Soc. Edinb. Earth Sci.* **77**, 99–125.

Mainprice, D. & Nicolas, A. 1989. Development of shape and lattice preferred orientations: application to the seismic anisotropy of the lower crust. *J. Struct. Geol.* **11**, 175–189.

Norris, R. J. & Bishop, D. G. 1990. Deformed conglomerates and textural zones in the Otago Schists, South Island, New Zealand. *Tectonophysics* **174**, 331–349.

Nyman, M. W., Law, R. D. & Smelik, E. A. 1992. Cataclastic deformation mechanism for the development of core-mantle structure in amphibole. *Geology* **20**, 455–458.

Ramsay, J. G. & Huber, M. I. 1983. *The Techniques of Modern Structural Geology, Volume 1: Strain Analysis*. Academic Press, London.

Rooney, T. P., Riecker, R. E. & Gavasci, A. T. 1975. Hornblende deformation features. *Geology* **3**, 364–366.

Rousell, D. H. 1981. Fabric and origin of gneissic layers in anorthositic rocks of the St. Charles Sill, Ontario. *Can. J. Earth. Sci.* **18**, 1681–1693.

Schwerdtner, W. M. 1964. Preferred orientation of hornblende in a banded hornblende gneiss. *Am. J. Sci.* **262**, 1212–1229.

Shelley, D. 1989. *P*, *M*, and *G* tectonites: a classification based on origin of mineral preferred orientations. *J. Struct. Geol.* **11**, 1039–1044.

Shelley, D. 1992. *Igneous and Metamorphic Rocks Under the Microscope*. Chapman & Hall, London.

Simpson, C. 1986. Determination of movement sense in mylonites. *J. Geol. Educ.* **34**, 246–261.

Tullis, J. & Yund, R. A. 1987. Transition from cataclastic flow to dislocation creep of feldspar: mechanisms and microstructures. *Geology* **15**, 606–609.

Van Den Driessche, J. & Brun, J. P. 1987. Rolling structures at large shear strain. *J. Struct. Geol.* **9**, 691–704.

Vernon, R. H. 1975. Deformation and recrystallisation of a plagioclase grain. *Am. Miner.* **60**, 884–888.

White, S. 1975. Tectonic deformation and recrystallisation of oligoclase. *Contr. Miner. Petrol.* **50**, 287–304.